Ab initio molecular dynamics study of the free surface of liquid Hg

L. Calderín,[1] L. E. González,[2] and D. J. González[2]

[1]*Materials Research Institute and Research Computing and Cyberinfrastructure, The Pennsylvania State University, Pennsylvania 16802, USA*

[2]*Departamento de Física Teórica, Universidad de Valladolid, 47011 Valladolid, Spain*

(Received 24 July 2012; revised manuscript received 12 October 2012; published 3 January 2013)

The free surface of liquid Hg at two temperatures has been studied by using first-principles molecular dynamics simulations. The longitudinal ionic density profile shows an oscillatory shape, and the wavelength of the oscillations is in good agreement with experiment. The associated self-consistent valence electronic density profile shows much weaker oscillations which are somewhat out of phase with the ionic ones. The calculated x-ray reflectivity shows a marked maximum at a wave-vector transfer of $q_z \approx 2.2$ Å^{-1}, whose origin is related to the surface layering.

DOI: 10.1103/PhysRevB.87.014201 PACS number(s): 61.25.Mv, 71.15.Pd

I. INTRODUCTION

In 1981 Rice and coworkers[1] predicted that the atomic density near the free surface of a metallic liquid would change in a nonmonotonic way, displaying a stratification in layers parallel to the interface. Moreover, those oscillations would show up as a Bragg-like peak in the x-ray (XR) reflectivity curve, $R(q_z)$, with the peak being located at a wave vector $q_z \approx 2\pi/\lambda$, where λ is the spacing between the layers.

However, it took several years to obtain the first experimental proof of surface layering. In 1995 Pershan and coworkers[2] reported the existence of surface layering in the free surface of liquid Hg (l-Hg) at room temperature. Since then, XR reflectivity measurements have been performed on other liquid-metal surfaces, such as Ga,[3] In,[4] K,[5] Sn,[6] and Bi;[7] in all cases, the measured XR reflectivity curves displayed (or suggested, as in the case of l-K) the expected Bragg-like peak.

From a theoretical standpoint, the nature of the mechanisms behind the surface layering phenomenon has not been elucidated yet, although several hypotheses have been advanced. Rice and coworkers[8] have pointed to the interconnection between the ionic and electronic densities and have noted that the rapid decay of the valence electronic density at the interface would generate a one-body energy whose gradient gives rise to a confining force that acts like a wall against which the ions are packed. Other explanations[9] have focused on the undercoordinated ions near the surface which would attempt to regain the coordination they had in the bulk liquid, resulting in an increased ionic density in the outermost liquid part and inducing the propagation of a density oscillation into the bulk. More recently, it has been proposed[10] that surface layering is a rather universal phenomenon which in most cases is frustrated by solidification, and therefore it only appears in those systems whose melting temperature is very low compared to the critical temperature. This latter suggestion has received some backing from a recent XR reflectivity experiment[11] where surface layering was found in a molecular nonmetallic liquid with a low melting point and a high critical point (as in a liquid metal), which suggests that the presence of an electron gas is not a basic condition in order to obtain an oscillating ionic density profile (DP). The oscillations in these types of systems are rather weak, showing values of the density maxima that are even smaller than the bulk density, in stark contrast to the strong oscillations found in liquid metals. Nevertheless, it was shown by Bomont *et al.*[12] that these strong oscillations can be obtained for liquids with a low melting temperature and a high critical temperature, provided that allowance is made for a change in the strength of the interactions (not in their form) across the liquid-vapor interface through a density dependence of this strength.

The experimental XR reflectivity data $R(q_z)$ have usually been analyzed by resorting to analytical models of the total electronic density profile (TEDP), which is the physical magnitude probed by the x rays. These analytical models include several parameters which are fitted in order to reproduce the measured $R(q_z)$ curve. The distorted crystal (DC) model has been the preferred model and has provided a reasonable fitting for the reflectivities of liquid Hg, Ga, In, and K.[2–5,13] However, some caution ought to be exercised when deriving an ionic DP from a measured $R(q_z)$, as it has been found that different DPs can lead to very similar $R(q_z)$ curves (see, for instance, Fig. 2 in Ref. 7). In addition to a model for the DP, it is also necessary to take into account how the thermally induced capillary waves in the surface affect the $R(q_z)$ data obtained in the measurement. This is usually done through the use of a Debye-Waller-type factor that includes a surface-roughness term. This term contains two contributions, one due to capillary waves, which is temperature dependent, and another one, called intrinsic, whose physical origin is not really well understood and which is, in principle, temperature independent.

Another route to calculate an ionic (or electronic) DP is by resorting to computer simulations, which provide a detailed description of the ionic positions and therefore allow the direct evaluation of the ionic DP. This method has been used by several authors, and their calculated ionic DPs have shown features very similar to those predicted by the DC model.[8,14–18]

This paper reports a computer simulation study on the surface structure of l-Hg, which has been performed by *ab initio* molecular dynamics (AIMD) simulations based on the density functional theory (DFT).[19] Given a collection of atoms with specified positions, DFT allows us to determine the ground-state electronic energy as well as the forces on the atoms. This approach provides the consistency between atomic and electronic properties, which is an essential requirement in regions of rapidly varying electron density, as is the case in free metallic surfaces. However, the computational burden

associated with the AIMD simulations is very heavy, which implies that the simulations can be performed for small samples (a few hundred particles) and for relatively short simulation times (few tens of picoseconds). This is the reason why very few AIMD studies have been performed to date, namely, for l-Si,[20] l-Na,[21] and l-Sn.[22]

As for the first experimental study of the free surface of l-Hg at room temperature,[2] we note that the measured $R(q_z)$ data were analyzed in terms of the DC model. The thus deduced TEDP showed a significant layering with a spacing of $\approx 3.05 \pm 0.15$ Å between the outer and the first inner layers and $\approx 2.76 \pm 0.20$ Å between all the other inner layers; moreover, the amplitude of the oscillations showed an exponential decay into the bulk. Subsequently, additional measurements[13] have been performed for several temperatures within the range 237–298 K. In order to explain the shape and the temperature variation of the measured $R(q_z)$ data, in Ref. 13 the authors made two important changes to the models used previously. First, in contrast to the first measurement, the DP was parametrized in terms of a DC model with the same distance between layers plus an additional Gaussian term located several angstroms into the vapor region and with a rather small density in the range 0.1–0.3 of the bulk value. Second, the intrinsic surface roughness had to be considered as temperature dependent, a feature that has not been observed in any other free liquid surface studied up to now.[3–5]

The first theoretical study on the free surface of l-Hg was carried out by Chekmarev *et al.*,[23] who performed Monte Carlo (MC) simulations based on density-dependent interatomic pair potentials obtained self-consistently within DFT and derived by using both local and nonlocal pseudopotentials. The study was done for three temperatures, namely, $T = 293$, 373, and 473 K, and the obtained results showed a marked oscillatory longitudinal ionic DP with a single wavelength which remained constant for all temperatures. The wavelength of the oscillations was $\lambda \approx 2.70$ and 2.85 Å for the local and nonlocal pseudopotentials, respectively, in reasonable agreement with the deduced experimental value for the inner layers.

Recently, Bomont *et al.*[12] have also studied the free surface of l-Hg for $T = 235$ and 293 K. They used MC simulations combined with a density-dependent effective interatomic potential, and the results showed an oscillatory longitudinal ionic DP whose wavelength was ≈ 2.6 Å. Their calculated reflectivity curves showed a qualitative agreement with experiment, although the main peak was somewhat shifted to greater q_z values.

II. COMPUTATIONAL METHOD

The AIMD calculations of the free surface of l-Hg were carried out in a slab geometry for two thermodynamic states characterized by temperatures $T = 300$ and 450 K and respective ionic number densities $\rho_i = 0.0403$ and 0.039 Å^{-3}. For each state, we considered a slab geometry with 116 atoms [i.e., $116 \times (10d + 2s,p) = 1392$ valence electrons] in a supercell with two free surfaces normal to the z axis. The dimensions of the slab were initially $L_x \times L_y \times L_z$, where $L_x = L_y = 13.03$ Å (for both temperatures) and $L_z = 17.1$ Å (300 K) and 18.0 Å (450 K). An additional 3.5 Å of vacuum were added along the z axis, above and below the slab, and periodic boundary conditions were used in all three space dimensions. Although the periodic boundary conditions require that a particle moving out of the cell in the z direction reappears on the other side of the cell, we have not observed this event during the simulations. Finally, we note that during its evolution the slab can contract or expand so as to achieve the zero external pressure condition; this allowed the above-mentioned input ionic number densities to change slightly during the calculations. For more details we refer the reader to Refs. 21 and 24–26.

During the simulations, the atomic configurations of the Hg ions in the system are generated under the Born-Oppenheimer approximation by solving the Kohn-Sham DFT equations[19] on a plane-wave basis set for a given configuration, calculating the forces on the ions using the Hellman-Feynman theorem, and solving the corresponding Newton's equations for constant total energy, as implemented in the QUANTUM ESPRESSO package.[27]

The electronic exchange-correlation energy has been described by using the local-density approximation as parametrized by Perdew and Zunger.[28] The ion-electron interaction has been described by means of an ultrasoft pseudopotential[29] which was generated from a scalar relativistic all-electron calculation of the atomic configuration [Xe] $(4f^{14})5d^{10}\,6s^2$ in the local-density approximation and including nonlinear core corrections.

The initial atomic positions within the slab were chosen at random, and the system was thermalized during 10 ps of simulation time. Therefrom, microcanonical AIMD simulations were performed over 8000 time steps, which amounted to 32 ps of simulation time. We have used a plane-wave representation with an energy cutoff of 25 Ry, and the single Γ point was used in sampling the Brillouin zone. This "sampling" is enough to obtain accurate forces, even though it is not enough for other electronic properties, such as the density of electronic states, which we do not address in this study. These 8000 configurations have been used in the evaluation of the properties. We stress that this computational scheme has recently been validated by its application to bulk l-Hg, for which we obtained a very accurate description of several static, dynamic, and electronic properties at several thermodynamic states, both near the triple point and in expanded states.[30,31]

III. RESULTS

The longitudinal ionic DP was computed from a histogram of the particle positions, and the obtained results are depicted in Figs. 1 and 2. The results display a marked stratification, with the amplitude of the oscillations being greater at the outer regions. First, we have checked that the previous stratification is not an artifact induced by the finite size of the simulation box. Therefore, we have computed the transverse ionic DPs, which have also been plotted in Figs. 1 and 2. Although they show clear oscillations, their amplitudes are substantially smaller than those of the longitudinal ionic DP.

For the state with $T = 300$ K, closer analysis of the layers reveals that the spacing between the outer and the first inner layers (as measured by the distance between the two consecutive maxima) is ≈ 2.95 Å, whereas for all the other

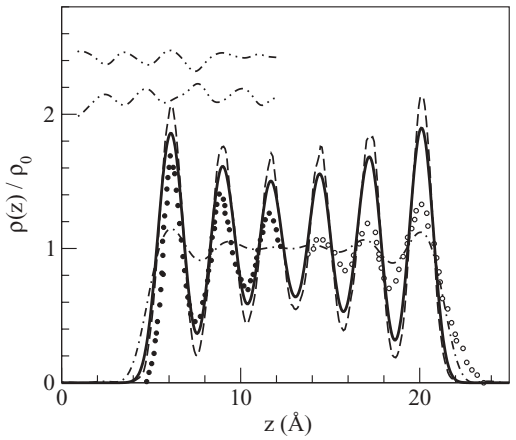

FIG. 1. Ionic (solid line), valence electronic (dash-dotted line), and total electronic (core plus valence; dashed line) DPs normal to the liquid-vapor interface of a liquid Hg slab at $T = 300$ K. The solid (open) circles represent the ionic DPs obtained by Chekmarev *et al.*[23] using a local (nonlocal) pseudopotential. All the densities have been plotted relative to the respective bulk values. The oscillating dash–double-dotted lines located at $\rho(z)/\rho_0 \approx 2.1$ and 2.4 are the x- and y-transverse ionic density profiles (displaced by arbitrary lengths), respectively.

inner layers the spacing is somewhat smaller, namely, ≈2.75 Å. We stress that these two distances are qualitatively in good agreement with the "experimental" results derived from the measured reflectivity data,[2] where, as mentioned previously, two different wavelengths were obtained. Comparison with all other previous theoretical calculations reveals that the present results are the first ones to account for the existence of two different wavelengths in the ionic DP of l-Hg. In addition, the present results clearly discard the model suggested in Ref. 13, where the DP was described by the DC model plus additional contributions located several angstroms towards the vapor side of the interface.

Figure 1 also includes the ionic DPs calculated by Chekmarev *et al.*[23] by using MC simulations combined with local and nonlocal pseudopotentials. These approaches predict a

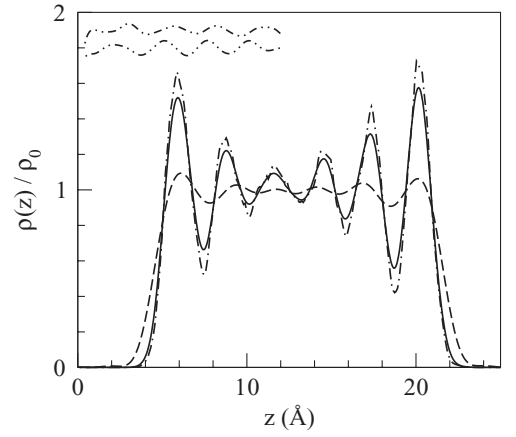

FIG. 2. Same as Fig. 1, but for $T = 450$ K. The oscillating dash–double-dotted lines located at $\rho(z)/\rho_0 \approx 1.8$ and 1.9 are the x- and y-transverse ionic density profiles (displaced by arbitrary lengths), respectively.

single interlayer spacing of ≈2.7 and ≈2.85 Å, respectively. The wavelength, amplitude, and decaying tail corresponding to the ionic DP associated with the local pseudopotential are much more similar to the present AIMD result than those derived using the nonlocal one. We notice that the "experimental" ionic DP obtained by using the DC model shows a slowly decaying broad tail which is not observed in the present AIMD results or in those of Chekmarev *et al.*[23]

As for the higher-temperature state ($T = 450$ K), our results for the longitudinal ionic DP show an oscillatory profile, with all the oscillations having the same wavelength of ≈2.90 Å. Note that when the temperature is increased, it has the effect of decreasing the amplitude of the oscillations in the longitudinal ionic DP while slightly increasing the wavelength of the inner oscillations.

In previous studies about the ionic DP in the free liquid surface of a wide range of simple liquid metals, we found a linear relationship between the wavelength λ of the ionic oscillations and the radii of the associated Wigner-Seitz spheres.[15] We have also ascertained that the relationship is also fulfilled by the previous calculated values of $\lambda = 2.75$ Å ($T = 300$ K) and 2.90 Å ($T = 450$ K).

The self-consistent valence electronic DP is also plotted in Figs. 1 and 2. For both temperatures, we observe some oscillations which are slightly out of phase with those of the ionic DP, although their amplitude is much smaller. In previous studies[15,16,22] concerning the relative phases of the ionic and valence electronic DPs, we have found that all possibilities are allowed, with the relative phase evolving from an opposite one, as happens for all the alkalis, to be almost in phase (Ga, In, Tl, Si, Sn).

In order to analyze the way various physical properties evolve when moving longitudinally along the slab, we have partitioned it into slices located between consecutive minima of the oscillatory longitudinal ionic DP, with the outer slice stretching from the outermost minimum to the point in the decaying tail where it takes half its bulk value. As shown in Figs. 1 and 2, the present AIMD results allow us to discern six slices. First, we have calculated the average ionic density within each slice. For both temperatures, the average ionic number density remains practically constant in the four inner slices, with a value which is ≈2% smaller than the corresponding input value (given in Sec. II). It is just at the outer slices where we observe an increase of ≈8% with respect to that of the central slices. This result compares well with the experimental value of ≈9% derived for the outer layer by using the DC model.[2] On the other hand, a density variation in the outer slice has also been obtained for other liquid metals,[16,22] where the average ionic density in the outer layer decreases in some cases (alkalis and alkali-earth metals) and increases in others (Al, Ga, In, Tl, Si, Sn).

Another interesting magnitude is the transverse pair distribution function $g_T(r)$ which describes the probability of finding two particles separated by a distance r when both particles are inside the layer. First, we have evaluated $g_T(r)$ inside the central section of the slab. In the case of a bigger slab with a greater number of slices, $g_T(r)$ can be calculated using several slices inside the central section, and the result should be very similar to the bulk pair distribution function.[16] However, in the present calculations, where the slab shows

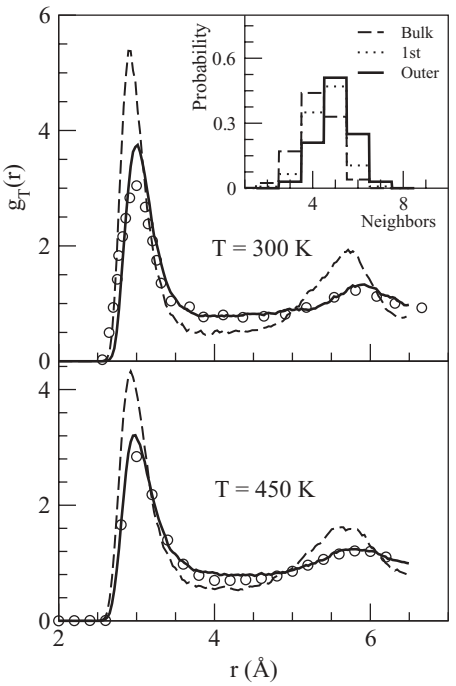

FIG. 3. Transverse pair correlation function for different layers at the free liquid surface of l-Hg at $T = 300$ and 450 K. The open circles stand for the bulk experimental data of Inui *et al.*[32] at $T = 300$ K and the data of Bosio *et al.*[33] at $T = 473$ K. The solid line is the $g_T(r)$ calculated at the two central layers, and the dashed line is that at the outermost layer. The inset at $T = 300$ K shows the distribution of the number of in-plane neighbors for different regions of the slab.

only six layers, we have calculated $g_T(r)$ inside the two central layers. This amounts to a 5.5-Å-wide (5.8-Å-wide) section for $T = 300$ K (450 K). Figure 3 depicts the calculated AIMD results, and we have also included a comparison with the experimental bulk data.[32,33] Despite the rather narrow region that could be considered in the calculation, the agreement with the experimental $g(r)$ is remarkable, with the calculated $g_T(r)$ closely following the characteristic features of the experimental data; in fact, the only discrepancy appears at $T = 300$ K, and it is related to the height of the main peak in $g_T(r)$, which is slightly overestimated. We consider that this good agreement corroborates the reliability of the present calculations. As for the outer layer, our results show that the corresponding $g_T(r)$ is slightly displaced towards smaller r values and its main peak is clearly higher than the bulk's. Interestingly, this is the same trend observed in liquid Al, Ga, Tl, Si, and Sn, with all of them showing some increase in the average ionic density of the outer layer.

Further insight into the three-dimensional local structure is provided by the z-dependent coordination number $n(z)$, defined as the average number of neighbors within a distance r_m taken as the position of the first minimum of the bulk radial distribution function $r^2 g_T(r)$; for both states, we have obtained that $r_m = 3.73$ Å. For $T = 300$ K, our results show that for most of the slab $n(z)$ remains practically constant [$n(z) \approx 9.4$], and it is very close to the surface, namely, around the outer slice, when $n(z)$ starts decreasing and reaches a value of $n(z) \approx 7.0$ at the position of the outer maximum. We recall that in a previous calculation[30] of bulk l-Hg at $T = 300$ K we obtained the same value of ≈9.4 for the number of nearest neighbors. At $T = 450$ K, $n(z) \approx 8.9$ for most of the slab, and it decreases at the outer maximum towards a value $n(z) \approx 7.0$. This ≈25% reduction is similar to what we have already found for a wide range a simple liquid metals.[16]

Next, we have proceeded to analyze the in-plane order within the slices, especially the outer slice for which different works have uncovered the predominance of five- and sixfold coordination. For example, MD simulations of supercooled Au surfaces[34] have found in the outer slice a preference of sixfold coordinated sites. Moreover, experimental[35] and AIMD[36] studies of l-Pb in contact with a solid Si wall have shown the existence of fivefold symmetry for the Pb atoms. Also, recent AIMD simulations of the free surface of l-Na[21] and l-Sn[22] have shown the predominance at the outer slice of fivefold coordinated atoms. Therefore, we have carried out a similar study for l-Hg at $T = 300$ K, and the obtained results are plotted as an inset in Fig. 3. The so-called bulk values have been obtained by using a slice with the same width as the outermost one but located at the center of the slab. The results show that in the outer slice, a fraction of approximately one-half of the atoms have fivefold coordination, although there are significant fractions of four- and sixfold coordinations too. Notice that when going inside the slab, there is an important reduction in the fractions of five- and sixfold coordinations along with a substantial increase in the fractions of three- and fourfold coordinations.

The XR reflectivity experiments performed on a free liquid surface probe the total electronic density, including core and valence electrons. In this technique, x rays of wavelength λ impinge upon the liquid surface at an angle α and are scattered at the same angle within the reflection plane defined by the incident beam and the surface normal. The reflected intensity $R(q_z)$ can be written as

$$\frac{R(q_z)}{R_F(q_z)} = |\Phi_{\rm int}(q_z)|^2 \, \exp\left(-\sigma_c^2 \, q_z^2\right), \qquad (1)$$

where $q_z = (4\pi/\lambda)\sin\alpha$ is the momentum transfer perpendicular to the interface, $R_F(q_z)$ is the Fresnel reflectivity of a perfectly sharp step-function interface, and $\Phi_{\rm int}(q_z)$ is the intrinsic surface structure factor, defined as

$$\Phi_{\rm int}(q_z) = \frac{1}{\rho_{e0}^T} \int_{-\infty}^{\infty} \left(\frac{\partial \rho_{e,\rm int}^T(z)}{\partial z} \right) \exp(i q_z z) \, dz, \qquad (2)$$

where ρ_{e0}^T is the average bulk total electronic (core plus valence) density and $\rho_{e,int}^T(z)$ is the *intrinsic* (i.e., in the absence of capillary wave smearing) longitudinal TEDP.

The exponential term in Eq. (1) is introduced to account for the effect of temperature on the longitudinal TEDP. This is made by representing the thermal excitations as capillary waves, with σ_c being an effective capillary wave roughness, which is usually written as

$$\sigma_c^2 = \sigma_0^2 + \sigma_{\rm cw}^2, \qquad (3)$$

where σ_0 represents an intrinsic surface roughness whose origin is not clear yet, although its inclusion has proved essential in order to properly describe the experimental reflectivity data.[3–5,13,17] The other term, $\sigma_{\rm cw}^2$, is the capillary wave theory result for the mean-square fluctuations in the

height-height correlation function.

$$\sigma_{\rm cw}^2 = \frac{k_B T}{2\pi\gamma}\ \ln\left(\frac{q_{\rm max}}{q_{\rm min}}\right), \tag{4}$$

where k_B stands for Boltzmann's constant, γ is the surface tension, and $q_{\rm max}$ and $q_{\rm min}$ are respectively the largest and smallest wave vector contributions to the thermal excitation of the interface. A usual choice is $q_{\rm max} = \pi/a$, with a being the ionic diameter, whereas $q_{\rm min}$ depends on the sample's size and also on the instrumental resolution.

A first step towards a full comparison with experimental data implies the construction of a longitudinal TEDP $\rho_e^T(z)$ from the AIMD simulations. This has been obtained by adding the self-consistent AIMD valence electronic DP and the total core electronic DP. This latter one was calculated by superposing, at the ionic sites, the associated core electronic density which was previously obtained by a Kohn-Sham DFT-type calculation. The core densities are rather narrow, and their superposition gives a longitudinal total core electronic DP in complete phase with the ionic one. Moreover, as the number of core electrons is much greater than that of valence electrons, the addition of the total core and valence electronic densities leads to a $\rho_e^T(z)$ whose phase practically coincides with that of the longitudinal ionic DP (see Figs. 1 and 2).

It must be noticed that the previously calculated $\rho_e^T(z)$ is not the intrinsic one because it includes those capillary waves corresponding to the temperature and the dimensions of the box used in the AIMD simulation. These fluctuations can be reasonably described in terms of an associated $\sigma_{\rm cw}^{\rm AIMD}$ defined as in Eq. (4). Therefore, a comparison with the experimental data will require us to properly account for these effects, and this is has been done as follows. From the calculated $\rho_e^T(z)$, we obtain the following expression for its associated reflected intensity:

$$\left[\frac{R(q_z)}{R_F(q_z)}\right]\ \exp\left(\sigma_0^2\ q_z^2\right)$$
$$= |\ \Phi(q_z)\ |^2 = \left|\frac{1}{\rho_{e0}}\int_{-\infty}^{\infty}\left(\frac{\partial\rho_e^T(z)}{\partial z}\right)\ \exp(iq_z z)\ dz\right|^2 . \tag{5}$$

Comparison with Eq. (1) shows that the AIMD calculated surface structure factor $\Phi(q_z)$ may be envisaged as the result of a convolution of the intrinsic one, $\Phi_{\rm int}(q_z)$, with an associated Gaussian distribution describing the thermal fluctuations in the simulation characterized by an effective capillary roughness $\sigma_{\rm cw}^{\rm AIMD}$. This has been evaluated according to Eq. (4), and we have used the values[37] $\gamma = 475$ mN/m (300 K), $\gamma = 445$ mN/m (450 K), and $q_{\rm max}$= 1.2 Å^{-1}, which is the same value used in the analysis of the experimental data.[2,13] As for $q_{\rm min}$, it is usually defined as $q_{\rm min} = \pi/L_0$, where L_0 stands for the square root of the slab's transverse area, and in the present AIMD simulations we have taken $q_{\rm min}^{\rm AIMD} = 0.24$ Å^{-1}. Using the previous values, we have obtained $\sigma_{\rm cw}^{\rm AIMD} = 0.47$ Å (300 K) and 0.60 Å (450 K). As for the intrinsic surface roughness σ_0 and because of its not well-defined status, we have chosen to perform calculations using different values within the range $0.20\ \text{Å} \leqslant \sigma_0 \leqslant 0.80$ Å.

On the other hand, when comparing with experimental reflectivity data, it must be noted that although $q_{\rm max}$ takes the same value in the experiment and the AIMD calculations, this is not the case for $q_{\rm min}$. Specifically, the experimental

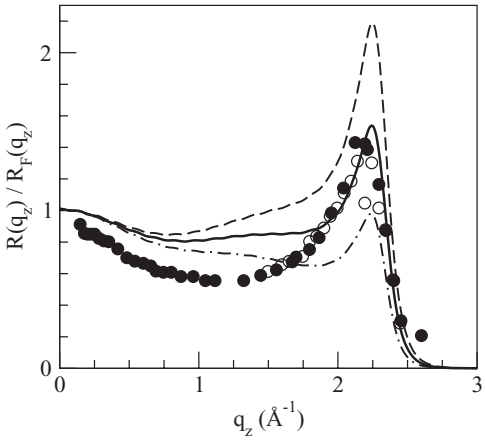

FIG. 4. Fresnel normalized reflectivity for liquid Hg at 300 K. The open and solid circles are the experimental data from Pershan and coworkers.[2,13] The lines are the present AIMD calculations using different values for the intrinsic surface roughness $\sigma_0 =$ 0.50 Å (dashed line), 0.40 Å (solid line), and 0.30 Å (dash-dotted line).

value[2,13] for $q_{\rm min}^{\rm Expt} = 0.0074$ Å^{-1}, which means that $\sigma_{\rm cw}^{\rm Expt} > \sigma_{\rm cw}^{\rm AIMD}$; i.e., the experiment includes a wider range of capillary waves. Indeed, using the above data, we have estimated that $\sigma_{\rm cw}^{\rm Expt} = 0.84$ (1.06) Å for $T = 300$ (450) K. So, in order to take this difference into account, i.e., to include the same range of capillary waves, the AIMD reflectivity has been computed as

$$\frac{R(q_z)}{R_F(q_z)} = |\Phi(q_z)|^2\ \exp\left\{-\left[(\sigma_0)^2 + \Delta\sigma_{\rm cw}^2\right] q_z^2\right\}, \tag{6}$$

where $\Delta\sigma_{\rm cw}^2 = (\sigma_{\rm cw}^{\rm Expt})^2 - (\sigma_{\rm cw}^{\rm AIMD})^2$; i.e., from the total capillary damping we subtract the contribution which is already included in the AIMD simulation.

Figure 4 shows the calculated AIMD reflectivity $R(q_z)/R_F(q_z)$ results for l-Hg at 300 K along with the corresponding experimental data.[2,13] We have plotted several curves calculated using different values for the intrinsic contribution σ_0. Although there is a marked dependence of the calculated reflectivity with respect to the value used for σ_0, we stress that all curves display a main peak whose position does not change and practically coincides with experiment, namely, $q_z \approx$ 2.2 Å^{-1}. Notice that this value for the peak's position correlates with the wavelength $\lambda = 2.75$ Å of the inner oscillations. The choice $\sigma_0 = 0.40$ Å provides a reasonable description of the experimental data, although it fails to reproduce the minimum centered around $q_z \approx 1.2$ Å^{-1}, as it also occurs with the other possible values of σ_0. Interestingly, we notice that the MC simulation results of Chekmarev *et al.*[23] when fitted to the DC model yielded a value $\sigma_0 = 0.37$ Å. Moreover, this value of σ_0 is comparable to those values we have obtained in similar studies we have carried out for Sn, Ga, In, and the Ga-In alloy.[17,18,22] The marked minimum exhibited by the experimental reflectivity, $R(q_z)/R_F(q_z)$, is a peculiar feature of l-Hg which has not been observed in the measured reflectivity curves of other liquid metals yet. We already mentioned that, in order to account for it, Pershan and coworkers[13] modeled the electronic DP in terms of the DC model plus an additional

Gaussian term located a few angstroms towards the vapor side of the interface. This suggestion is not supported by the present AIMD calculations, which, on the contrary, favor the model used in the first experiment[2] with a denser outer layer and an increased interlayer distance with respect to the inner ones.

The AIMD data do not reproduce the dip in the reflectivity, and we tentatively ascribe this discrepancy with experiment to the reduced number of layers that can be afforded in the theoretical calculation due to computational demands. In this respect it would be highly desirable to include more particles in the study by using schemes, such as the orbital-free DFT,[16] that alleviate the computational burden while still keeping a good accuracy. However, this would require the development of local pseudopotentials and kinetic energy functionals able to cope with complicated metals like Hg, where *d* electrons can play an important role. Finally, we mention that we have not depicted the calculated reflectivity results for $T = 450$ K because the reflectivity curve shows a monotonically decreasing behavior with no additional relevant features.

IV. CONCLUSIONS

We have reported results of *ab initio* simulations for the free liquid surface of l-Hg at two temperatures. The calculated longitudinal ionic DP exhibits surface layering whose amplitude decreases with increasing temperature. The result for $T = 300$ K shows that the spacing between the outer and the first inner layers (≈2.95 Å) is somewhat greater than that between the inner layers (≈2.75 Å). Moreover, the outer layer has a mean ionic density which is ≈8% greater than that of the central slices. These results compare rather well with the features of the ionic DP derived from the "experimental" reflectivity data.[2]

The longitudinal valence electronic DP also exhibits (weaker) oscillations which are slightly out of phase with the ionic ones. We have calculated the total electronic DP, which stands practically in phase with the ionic DP, and therefrom we have proceeded to evaluate the associated XR reflectivity, which is the magnitude experimentally measured. This calculation requires us to include the effect of the thermal excitations, which has been achieved by means of a Debye-Waller-type factor whose main ingredient is an effective capillary wave roughness parameter. This parameter has two contributions, with one of them, the so-called intrinsic surface roughness, still lacking a clear physical interpretation. The calculated reflectivity shows a main peak whose position and width are in qualitative agreement with experiment; however, the calculated reflectivity does not properly reproduce the extended minimum at around $q_z \approx 1.2$ Å^{-1}. Given the *ab initio* nature of the present calculations, we think that this failure is likely to be induced by the small number of layers affordable in the calculation. Extension to larger simulation samples is important, even if additional approximations have to be included, and work along these lines is in progress.

ACKNOWLEDGMENTS

L.C. acknowledges the financial support of the University of Valladolid. L.E.G. acknowledges the support of the MCINN in conjunction with FEDER funds (Grant No. FIS2011-22957) and JCyL (Grant No. VA104A11-2). D.J.G. gratefully acknowledges the financial support of MECD (Grant No. PR2011-0019).

[1] M. P. D'Evelyn and S. A. Rice, Phys. Rev. Lett. **47**, 1844 (1981).
[2] O. M. Magnussen, B. M. Ocko, M. J. Regan, K. Penanen, P. S. Pershan, and M. Deutsch, Phys. Rev. Lett. **74**, 4444 (1995).
[3] M. J. Regan, E. H. Kawamoto, S. Lee, P. S. Pershan, N. Maskil, M. Deutsch, O. M. Magnussen, B. M. Ocko, and L. E. Berman, Phys. Rev. Lett. **75**, 2498 (1995).
[4] H. Tostmann, E. DiMasi, P. S. Pershan, B. M. Ocko, O. G. Shpyrko, and M. Deutsch, Phys. Rev. B **59**, 783 (1999).
[5] O. G. Shpyrko, P. Huber, A. Y. Grigoriev, P. S. Pershan, B. Ocko, H. Tostmann, and M. Deutsch, Phys. Rev. B **67**, 115405 (2003).
[6] O. G. Shpyrko, A. Y. Grigoriev, C. Steimer, P. S. Pershan, B. Lin, M. Meron, T. Graber, J. Gerbhardt, B. Ocko, and M. Deutsch, Phys. Rev. B **70**, 224206 (2004).
[7] P. S. Pershan, S. E. Stoltz, O. G. Shpyrko, M. Deutsch, V. S. K. Balagurusamy, M. Meron, B. Lin, and R. Streitel, Phys. Rev. B **79**, 115417 (2009).
[8] M. Zhao, D. S. Chekmarev, Z.-H. Cai, and S. A. Rice, Phys. Rev. E **56**, 7033 (1997); D. Chekmarev, M. Zhao, and S. A. Rice, J. Chem. Phys. **109**, 1959 (1998).
[9] S. Iarlori, P. Carnevali, F. Ercolessi, and E. Tosatti, Surf. Sci. **211-212**, 55 (1989).
[10] E. Chacón, M. Reinaldo-Falagan, E. Velasco, and P. Tarazona, Phys. Rev. Lett. **87**, 166101 (2001); E. Velasco, P. Tarazona, M. Reinaldo-Falagan, and E. Chacón, J. Chem. Phys. **117**, 10777 (2002).
[11] H. Mo, G. Evmenenko, S. Kewalramani, K. Kim, S. N. Ehrlich, and P. Dutta, Phys. Rev. Lett. **96**, 096107 (2006).
[12] J. M. Bomont, J. L. Bretonnet, D. J. González, and L. E. González, Phys. Rev. B **79**, 144202 (2009).
[13] E. DiMasi, H. Tostmann, B. M. Ocko, P. S. Pershan, and M. Deutsch, Phys. Rev. B **58**, R13419 (1998).
[14] D. J. González, L. E. González, and M. J. Stott, Phys. Rev. Lett. **92**, 085501 (2004); **94**, 077801 (2005).
[15] L. E. González, D. J. González, and M. J. Stott, J. Chem. Phys. **123**, 201101 (2005).
[16] D. J. González, L. E. González, and M. J. Stott, Phys. Rev. B **74**, 014207 (2006).
[17] D. J. González and L. E. González, J. Phys. Cond. Matter **20**, 114118 (2008).
[18] L. E. González and D. J. González, Phys. Rev. B **77**, 064202 (2008).
[19] P. Hohenberg and W. Kohn, Phys. Rev. **136**, 864 (1964); W. Kohn and L. J. Sham, *ibid.* **140**, A1133 (1965).
[20] G. Fabricius, E. Artacho, D. Sanchez-Portal, P. Ordejon, D. A. Drabold, and J. M. Soler, Phys. Rev. B **60**, R16283 (1999).
[21] B. G. Walker, C. Molteni, and N. Marzari, J. Phys Condens. Matter **16**, S2575 (2004); J. Chem. Phys. **124**, 174702 (2006); **127**, 134703 (2007).
[22] L. Calderín, L. E. González, and D. J. González, Phys. Rev. B **80**, 115403 (2009).

[23]D. S. Chekmarev, M. Zhao, and S. A. Rice, Phys. Rev. E **59**, 479 (1999).
[24]E. Salomons and M. Mareschal, J. Phys Condens. Matter **3**, 3645 (1991).
[25]S. W. Sides, G. S. Grest, and M.-D. Lacasse, Phys. Rev. E **60**, 6708 (1999).
[26]L. Calderín, L. E. González, and D. J. González, Phys. Rev. B **80**, 115403 (2009).
[27]S. Baroni, A. Dal Corso, S. de Gironcoli, P. Giannozzi, C. Cavazzoni, G. Ballabio, S. Scandolo, G. Chiarotti, P. Focher, A. Pasquarello, K. Laasonen, A. Trave, R. Car, N. Marzari, and A. Kokalj, QUANTUM ESPRESSO, http://www.pwscf.org/.
[28]D. M. Ceperley and B. J. Alder, Phys. Rev. Lett. **45**, 566 (1980); J. P. Perdew and A. Zunger, Phys. Rev. B **23**, 5048 (1981).
[29]D. Vanderbilt, Phys. Rev. B **41**, 7892 (1990).
[30]L. Calderín, L. E. González, and D. J. González, J. Chem. Phys. **130**, 194505 (2009).
[31]L. Calderín, L. E. González, and D. J. González, J. Phys. Cond. Matter **23**, 375105 (2011).
[32]M. Inui, X. Hong, and K. Tamura, Phys. Rev. B **68**, 094108 (2003).
[33]L. Bosio, R. Cortes, and C. Segaud, J. Chem. Phys. **71**, 3595 (1979).
[34]F. Celestini, F. Ercolessi, and E. Tosatti, Phys. Rev. Lett. **78**, 3153 (1997).
[35]H. Reichert, O. Klein, H. Dosch, M. Denk, V. Honkimaki, T. Lippmann, and G. Reiter, Nature (London) **408**, 839 (2000).
[36]J. Souto, M. M. G. A. Alemany, R. C. Longo, L. J. Gallego, L. E. González, and D. J. González, Phys. Rev. B **82**, 134118 (2010).
[37]T. Iida and R. I. L. Guthrie, in *The Physical Properties of Liquid Metals* (Clarendon, Oxford, 1988), p. 133.